Preprints of the 19th World Congress
The International Federation of Automatic Control
Cape Town, South Africa. August 24-29, 2014

On the feedforward control problem for discretized port-Hamiltonian systems

Paul Kotyczka *

* *Institute of Automatic Control, Technische Universität München, 85748 Garching, Germany, E-mail: kotyczka@tum.de.*

Abstract: The boundary feedforward control problem for a class of distributed-parameter port-Hamiltonian systems in one spatial dimension is addressed. The considered hyperbolic systems of two conservation laws (with dissipation) are discretized in the spatial coordinate using an energy-based, structure preserving discretization scheme. The resulting finite-dimensional approximate state representation has a feedthrough term which allows to directly express the differential equation for the inverse dynamics. The inverse system needs to be solved in order to determine the control inputs for given desired output trajectories. For non-collocated pairs of boundary in- and outputs the magnitude of dissipation determines whether the inverse discretized models are stable or not. In the unstable case, the problem at hand can be attacked with classical approaches for the dynamic inversion of non-minimum phase systems.

Keywords: Infinite-dimensional systems, port-Hamiltonian systems, structure preserving discretization, dynamic inversion.

1. INTRODUCTION

The port-Hamiltonian approach is an elegant way to formulate nonlinear, energy-based models of multi-domain physical systems. The equations describing a port-Hamiltonian (pH) dynamical system have an intuitive structure, where each of the containing symbols is related to the stored energy, its exchange between different types and subsystems, and its dissipation, see van der Schaft (2000). This holds not only in the finite-dimensional case, but also for infinite-dimensional systems, governed by systems of partial differential equations (van der Schaft and Maschke, 2002). The pH structure can be exploited, for example, to design finite-dimensional energy-shaping feedback controllers for infinite-dimensional systems, based on the construction of structural invariants (Casimir functions) for the closed-loop system (Macchelli and Melchiorri, 2005; Schöberl and Siuka, 2013). The limiting factor for the application of these methods, however, is the presence of physical dissipation.

In general, analysis and controller design become more tractable when a finite-dimensional approximation (by spatial discretization) of the infinite-dimensional system is used. In Golo et al. (2004), a technique has been introduced to obtain such an approximation preserving the port-Hamiltonian structure. In particular, the physical property of passivity of the original system is preserved in the approximation. Examples of related approaches for structure preserving discretization are Moulla et al. (2012) or Farle et al. (2013). An advantage of pH discretization is that nonlinearities, which originate in a non-quadratic energy functional [1], and which may have a dominant effect on the system dynamics, are preserved in the discretized model. A finite-dimensional pH model of lower dimension used for feedforward controller design, might suffice in order to achieve satisfactory tracking performance, compared to a higher dimensional linear approximation, for example.

The systems considered in this paper are hyperbolic systems of two conservation laws with dissipation [2]. This includes the simplest linear case of an electric transmission line with quadratic energy and constant parameters, but also nonlinear systems like hydraulic/pneumatic flows in pipes, nano scale transmission lines with varying geometric properties or non-quadratic energy terms, or the shallow water equations for flows in open channels.

The feedforward control problem for discretized port-Hamiltonian systems of this type is addressed. Given desired output trajectories, the corresponding inputs shall be determined. The solution of

⋆ The author is with the Institute of Automatic Control (Prof. Boris Lohmann).

[1] This includes also spatial integrals over a quadratic form with non-constant Hessian.

[2] Inspired by the electric example, the class of systems is for brevity called (general) *transmission systems*.

this task depends on (non-)collocation of in- and outputs. In the case of collocated in-/outputs [3] the problem is solved by numerical integration of the stable inverse dynamics, which is the dual state representation with in- and outputs permuted. When in- and outputs are non-collocated [4] stability of the inverse dynamics is lost in general and (numerical) methods for the stable inversion of non-minimum phase systems need to be applied.

The remainder of the paper is organized as follows. In Section 2, the considered infinite-dimensional models of transmission systems are presented. Section 3 contains a brief summary of structure preserving discretization and the derivation of the different finite-dimensional models considered in the paper. In Section 4, the inverse models are presented and in Section 5, the feedforward control problem is analyzed for collocated and non-collocated in- and outputs, respectively. A condition is given for stable dynamic inversion in the case of non-collocation. A summary and future research perspectives conclude the paper in Section 6.

2. INFINITE-DIMENSIONAL MODELS

In this section, the class of hyperbolic systems of two conservation laws (transmission systems) is introduced and illustrated at the examples of the linear transmission line and the nonlinear flow in open channels (shallow water equations). The unified port-Hamiltonian model is presented and the different possibilities for boundary in- and outputs are discussed.

2.1 Physical examples

Transmission line. The transient behavior of a single electric transmission line (or a pair of transmission lines, respectively) is governed by the hyperbolic linear partial differential equations

$$\begin{aligned} \partial_t(li(x,t)) &= -\partial_x v(x,t) - ri(x,t) \\ \partial_t(cv(x,t)) &= -\partial_x i(x,t) - gv(x,t). \end{aligned} \tag{1}$$

$\psi(x,t) = li(x,t)$ and $q(x,t) = cv(x,t)$ are the distributed magnetic flux and electric charge densities, $i(x,t)$ and $v(x,t)$ the current and the voltage. l and c are the series inductance and parallel capacitance, r an g denote the resistance and admittance, each per unit length, x is the spatial coordinate.

For the linear transmission line, analytic expressions exist to compute the voltage (current) at one terminal from voltage and current signals at the other terminal (Fliess et al., 1999). In Schmuck et al. (2014) these expressions are used to solve the feedforward control problem in a network of HVDC transmission lines.

[3] i. e. when in- and output are a pair of conjugate power variables at one terminal of the system

[4] i. e. physical quantities of same type at opposite terminals

Shallow water equations. The transient flow in an open channel with constant width can be described by the one-dimensional shallow water or Saint Venant equations [5]

$$\begin{aligned} \partial_t h &= -\partial_x(hv) \\ \partial_t v &= -v\partial_x v - g\partial_x h + g(S_0 - S_f) \end{aligned} \tag{2}$$

with the water level $h(x,t)$ and the flow velocity $v(x,t)$ as distributed states. The remaining quantities are the gravitational acceleration g, the channel bottom slope S_0 and the so-called friction slope S_f

$$S_0(x) = -\partial_x b(x), \quad S_f(x,t) = \frac{Cv(x,t)|v(x,t)|^{m-1}}{R^p}, \tag{3}$$

where $b(x)$ is the bottom height, C a friction coefficient, R the hydraulic radius, and m, p parameters depending on the flow regime. In Knüppel et al. (2010), where Eqs. (2) and (3) are taken from, a trajectory generation approach for the shallow water equations is proposed, based on numerical integration along the characteristics of the PDEs. Hamroun et al. (2006) present the structure preserving discretization and simulation of the shallow water equations. In Pasumarthy and van der Schaft (2006) the discretized model is derived, where in addition the fluid velocity component, perpendicular to the main flow direction is considered.

2.2 Unified port-Hamiltonian model

Both electric and fluidic model can be represented in a unified way with the following distributed-parameter pH state representation (including dissipation), see e. g. van der Schaft (2006):

$$\begin{bmatrix} \partial_t z_1 \\ \partial_t z_2 \end{bmatrix} = \begin{bmatrix} 0 & -1 \\ -1 & 0 \end{bmatrix} \begin{bmatrix} \partial_x e_1 \\ \partial_x e_2 \end{bmatrix} - \begin{bmatrix} r_1 & 0 \\ 0 & r_2 \end{bmatrix} \begin{bmatrix} e_1 \\ e_2 \end{bmatrix}. \tag{4}$$

$\boldsymbol{z}(x,t) = [z_1(x,t) \;\; z_2(x,t)]^T$ denotes the vector of distributed state variables and $\boldsymbol{e}(x,t) = [e_1(x,t) \;\; e_2(x,t)]^T$ represents the vector of distributed efforts (co-states), which are defined as the variational derivatives of the energy functional on the considered spatial interval [6]:

$$\boldsymbol{e}(x,t) = (\delta_z H(\boldsymbol{z}))^T. \tag{5}$$

The time derivatives of the states $\boldsymbol{f}(x,t) = \dot{\boldsymbol{z}}(x,t)$ are called flows. Together with the efforts, they define a pair of conjugated power variables. $r_i(x) \geq 0$, $i = 1, 2$, are distributed dissipation coefficients. The energy stored on the spatial interval $[0, L]$ is given by a functional

$$H(\boldsymbol{z}) = \int_0^L \mathcal{H}(\boldsymbol{z}(x,t))\, dx, \tag{6}$$

where $\mathcal{H}(\boldsymbol{z}(x,t))$ denotes the energy or Hamiltonian density. The row vector of variational derivatives $\delta_z H$ of H is defined by the relation

[5] Arguments of functions are dropped, when they are clear from the context.

[6] Notation: $\partial_z H$ (∇H) denotes the row (column) vector of partial derivatives of a function $H(\boldsymbol{z})$. Likewise, $\delta_z H$ is the row vector of variational derivatives of a functional $H(\boldsymbol{z}(x))$.

Table 1. Variables in the transmission line example (densities per unit length)

Var.	Physical quantity	
z_1	ψ	flux density
z_2	q	charge density
$\mathcal{H}$	$\frac{1}{2l}\psi^2 + \frac{1}{2c}q^2$	mag. plus el. energy density
e_1	i	current
e_2	v	voltage
r_1	r	resistance per unit length
r_2	g	admittance per unit length

Table 2. Variables in the shallow water example, ρ: density of water

Var.	Physical quantity	
z_1	v	flow velocity
z_2	h	water height
$\mathcal{H}$	$\frac{1}{2}(hv^2 + gh^2 + 2hgb(x))$	Energy per area per ρ
e_1	vh	volumetric flow, divided by channel width
e_2	$\frac{1}{2}v^2 + gh + gb(x)$	Total pressure per ρ
r_1	$\frac{gC\lvert v\rvert^{m-1}}{hR^p}$	friction coefficient

$$H(\boldsymbol{z} + \varepsilon\boldsymbol{\eta}) = H(\boldsymbol{z}) + \varepsilon \int_0^L \delta_z H \boldsymbol{\eta}\, dx + \mathcal{O}(\varepsilon^2) \quad (7)$$

with ε small and $\boldsymbol{\eta}$ a vector of smooth functions such that $\boldsymbol{z} + \varepsilon\boldsymbol{\eta}$ satisfies the same boundary conditions as $\boldsymbol{z}$. In case the energy (Hamiltonian) density $\mathcal{H}$ does not depend on spatial derivatives of the states, the variational derivatives of H can be identified with the partial derivatives of the energy density: $\delta_z H = \partial_z \mathcal{H}$. With $\varepsilon = dt$, $\boldsymbol{\eta} = \dot{\boldsymbol{z}}$, the time derivative of H can be expressed as

$$\begin{aligned}\dot{H} &= \int_0^L \delta_z H \dot{\boldsymbol{z}}\, dx = \quad (8)\\ &= \int_0^L \boldsymbol{e}^T \begin{bmatrix} 0 & -1 \\ -1 & 0 \end{bmatrix} \partial_x \boldsymbol{e}\, dx - \int_0^L \boldsymbol{e}^T \begin{bmatrix} r_1 & 0 \\ 0 & r_2 \end{bmatrix} \boldsymbol{e}\, dx.\end{aligned}$$

Integration by parts yields the energy balance equation for the infinite-dimensional pH system

$$\dot{H} \leq e_1(0)e_2(0) - e_1(L)e_2(L). \quad (9)$$

The energy balance equation results from the fact that flows and efforts associated to distributed energy storage and dissipation, as well as energy exchange through the boundary, are related by a power-conserving interconnection. The latter can be formalized by a so-called Stokes-Dirac structure (van der Schaft and Maschke, 2002).

Tables 1 and 2 contain the definitions of the variables in the pH model for both physical examples.

2.3 Boundary conditions

The state representation of a distributed-parameter system is completed with the definition of boundary conditions. For the considered class of systems with two states, distributed along one spatial dimension, boundary conditions are imposed on the effort variables at the terminals of the transmission system ($x = 0$ and $x = L$, respectively). In this paper, the following cases are distinguished.

Collocated in-/output pairs. Two efforts of different type, one at each terminal, are considered as control inputs, while the conjugate [7] efforts are considered as outputs. One possible combination is

$$\begin{bmatrix} u_1 \\ u_2 \end{bmatrix} = \begin{bmatrix} e_2(0) \\ -e_1(L) \end{bmatrix}, \quad \begin{bmatrix} y_1 \\ y_2 \end{bmatrix} = \begin{bmatrix} e_1(0) \\ e_2(L) \end{bmatrix}. \quad (10)$$

The minus sign ensures that $\boldsymbol{y}^T\boldsymbol{u}$ is the power *supplied* to the system through the boundary. This definition of in- and outputs is shown in Fig. 1 for the transmission line example. Another possibility, where simply the roles of inputs and collocated outputs are changed, is

$$\begin{bmatrix} u_1' \\ u_2' \end{bmatrix} = \begin{bmatrix} e_1(0) \\ e_2(L) \end{bmatrix}, \quad \begin{bmatrix} y_1' \\ y_2' \end{bmatrix} = \begin{bmatrix} e_2(0) \\ -e_1(L) \end{bmatrix}. \quad (11)$$

Non-collocated in-/output pairs. Effort variables of same type (e. g. voltages) at opposite terminals form a pair of non-collocated in- and outputs, like

$$\begin{bmatrix} \tilde{u}_1 \\ \tilde{u}_2 \end{bmatrix} = \begin{bmatrix} e_2(0) \\ e_1(0) \end{bmatrix}, \quad \begin{bmatrix} \tilde{y}_1 \\ \tilde{y}_2 \end{bmatrix} = \begin{bmatrix} e_2(L) \\ -e_1(L) \end{bmatrix}. \quad (12)$$

Effect of terminal resistance. By an algebraic relation between the efforts at one terminal, e. g. due to an ohmic terminal load in the electric example, the number of (free) control inputs and outputs of the pH system is reduced. At $x = L$ (index "L") this relation can be expressed as

$$e_2(L) = R_L(\boldsymbol{z}(L))e_1(L), \quad (13)$$

where R_L is a, possibly state dependent, lumped resistive term. For the transmission line, an ohmic load at $x = L$ is modeled by

$$v_L = R_L i_L \quad \Leftrightarrow \quad e_2(L) = R_L e_1(L). \quad (14)$$

For the shallow water equations, at the downstream end of the channel section a weir with a discharge characteristics (Knüppel et al., 2010)

$$Q_w = h_L v_L = C_w \frac{2}{3}\sqrt{2g}(h_L - w)^{\frac{3}{2}} \quad (15)$$

is assumed (height w, discharge coefficient C_w). Squaring this equation, dividing by $2h_L^2$ and adding $gh_L + gb_L$, one obtains

$$\frac{1}{2}v_L^2 + gh_L + gb_L = \frac{\frac{4}{9}C_w g(h_L - w)^3 + gh_L^3}{h_L^2} + gb_L. \quad (16)$$

Setting $b_L = 0$, as a reference level for the channel bottom height, the equation can be rearranged:

$$\underbrace{\frac{1}{2}v_L^2 + gh_L}_{e_2(L)} = \underbrace{\frac{4C_w g}{9v_L}\left(1 + \frac{(h_L - w)^3}{h_L^3}\right)}_{R_L(z_1(L), z_2(L))} \underbrace{h_L v_L}_{e_1(L)}. \quad (17)$$

[7] The product of an effort variable with its conjugate counterpart has the unit of power.

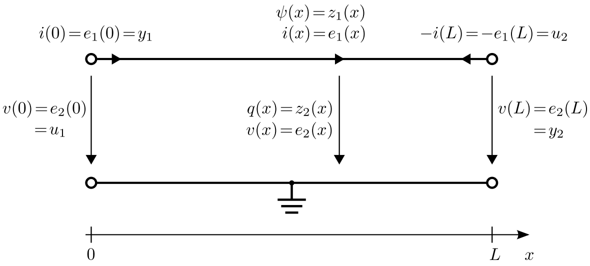

Fig. 1. Distributed states, efforts, in- and outputs in the transmission line example.

The effect of the weir corresponds to a state-dependent terminal resistance.

3. DISCRETIZED MODELS

The goal of structure preserving spatial discretization of infinite-dimensional pH systems is to obtain a finite-dimensional approximate model in pH form, which obeys the energy balance equation (9). In this section, the discretization scheme according to Golo et al. (2004) is summarized with the simplest possible shape functions and it is shown how to construct N-segment models of the considered transmission systems. The discretized models are given for the cases of collocated and non-collocated in-/outputs as well as for the non-collocated SISO case with terminal resistance.

3.1 Discretization of states and efforts

The distributed states $z_i(x,t)$ and efforts $e_i(x,t)$, $i=1,2$ on an interval $x \in [a,b]$ are approximated by

$$z_i(x,t) \approx Z_i(t)\omega_i^{ab}(x) \tag{18}$$

$$e_i(x,t) \approx E_i^a(t)\omega_i^a(x) + E_i^b(t)\omega_i^b(x). \tag{19}$$

$Z_i(t)$ are the states of the discretized model and the boundary efforts $E_i^{a/b}(t)$ will serve as in- and outputs. The shape functions [8] $\omega_i^{ab}(x)$ and $\omega_i^a(x)$, $\omega_i^b(x)$ have to be chosen such that the $Z_i(t)$ approximate the integrals of the distributed states while $E_i^{a/b}(t)$ reproduce the boundary efforts of the infinite-dimensional system:

$$Z_i(t) \approx \int_a^b z_i(x,t)\,dx \tag{20}$$

$$E_i^a(t) \approx e_i(a,t), \qquad E_i^b(t) \approx e_i(b,t). \tag{21}$$

These requirements translate into the conditions

$$\int_a^b \omega_i^{ab}(x)\,dx = 1, \tag{22}$$

$$\omega_i^a(a) = \omega_i^b(b) = 1, \quad \omega_i^a(b) = \omega_i^b(a) = 0. \tag{23}$$

Replacing (18) and (19) in the partial differential equations (4), where for the moment the dissipation is ignored, i. e. $r_1 = r_2 = 0$ is assumed, yields

$$\begin{aligned} \omega_1^{ab}(x)\dot{Z}_1(t) &= -\partial_x\omega_2^a(x)E_2^a(t) + \partial_x\omega_2^b(x)E_2^b(t) \\ \omega_2^{ab}(x)\dot{Z}_2(t) &= -\partial_x\omega_1^a(x)E_1^a(t) + \partial_x\omega_1^b(x)E_1^b(t). \end{aligned} \tag{24}$$

The simplest choice of shape functions such that the terms depending on x cancel in (24) is ($i = 1,2$)

$$\omega_i^{ab} = \frac{1}{b-a}, \qquad \omega_i^a(x) = \frac{b-x}{b-a}, \quad \omega_i^b(x) = \frac{x-a}{b-a}. \tag{25}$$

What remains is the set of two ordinary differential equations, excited by the boundary efforts

$$\begin{aligned} \dot{Z}_1(t) &= -E_2^a(t) + E_2^b(t) \\ \dot{Z}_2(t) &= -E_1^a(t) + E_1^b(t). \end{aligned} \tag{26}$$

The average effort variables on one segment are defined as

$$E_i(t) = \frac{1}{2}(E_i^a(t) + E_i^b(t)). \tag{27}$$

3.2 One-segment model

Choosing the in- and outputs according to Eq. (10), at the boundaries a and b (instead of 0 and L)

$$\begin{bmatrix} U_1 \\ U_2 \end{bmatrix} = \begin{bmatrix} E_2^a \\ -E_1^b \end{bmatrix} \approx \begin{bmatrix} e_2(a) \\ -e_1(b) \end{bmatrix}, \quad \begin{bmatrix} Y_1 \\ Y_2 \end{bmatrix} = \begin{bmatrix} E_1^a \\ E_2^b \end{bmatrix} \approx \begin{bmatrix} e_1(a) \\ e_2(b) \end{bmatrix}, \tag{28}$$

and approximating the effect of dissipation by the terms $-R_i(\boldsymbol{Z})E_i$ with

$$R_i(\boldsymbol{Z}) = (b-a)r_i(\frac{\boldsymbol{Z}}{b-a}), \tag{29}$$

see the remark below, the discretized pH state representation for one segment (superscript “1”) is

$$\begin{aligned} \dot{\boldsymbol{Z}} &= (\boldsymbol{J}^1 - \boldsymbol{R}^1)\boldsymbol{E} + \boldsymbol{G}^1\boldsymbol{U} \\ \boldsymbol{Y} &= (\boldsymbol{G}^1)^T\boldsymbol{E}(t) + \boldsymbol{D}^1\boldsymbol{U} \end{aligned} \tag{30}$$

with

$$\begin{aligned} \boldsymbol{F}^1 &= \boldsymbol{J}^1 - \boldsymbol{R}^1 = \begin{bmatrix} -R_1(\boldsymbol{Z}) & -2 \\ 2 & -R_2(\boldsymbol{Z}) \end{bmatrix}, \\ \boldsymbol{G}^1 &= [\boldsymbol{g}_1^1\ \boldsymbol{g}_2^1] = \begin{bmatrix} 2 & 0 \\ 0 & 2 \end{bmatrix}, \quad \boldsymbol{D}^1 = \begin{bmatrix} 0 & 1 \\ -1 & 0 \end{bmatrix}. \end{aligned} \tag{31}$$

The vector of efforts $\boldsymbol{E}$ is indeed the gradient $\nabla_Z H_{ab}$ of the approximate energy on the interval $[a,b]$ of the transmission system,

$$H_{ab} = (b-a)\mathcal{H}(\frac{\boldsymbol{Z}}{b-a}) \approx \int_a^b \mathcal{H}(\boldsymbol{z}(x))dx. \tag{32}$$

Remark 1. The explicit one-segment discretized pH model for the shallow water equations was derived in Pasumarthy and van der Schaft (2006).

Remark 2. To match the dissipated power in the discretized model, it is required that

$$\int_a^b r_i e_i^2(x)\,dx \approx R_i E_i^2, \quad i = 1,2. \tag{33}$$

Replacing (19) under the integral and using the definition of average efforts (27), expressions of the boundary efforts remain on the left hand side. The effect of these terms diminishes with the number of segments interconnected in series, such that (29) is a valid approximation of the dissipation.

[8] While $\omega_i^{a/b}$ are indeed functions (0-forms), it is evident from Eq. (22) that the “shape functions” $\omega_i^{ab}(x)$ are differential 1-forms.

3.3 Series interconnection

For the series interconnection of two segments on the intervals $[a_k, b_k]$, $[a_{k+1}, b_{k+1}]$, the conditions

$$E_i^{b_k} = E_i^{a_{k+1}}, \quad i = 1, 2 \tag{34}$$

have to be obeyed. With the definition of collocated in- and outputs according to Eq. (10), this means

$$U_1^{k+1} = Y_2^k, \qquad U_2^k = -Y_1^{k+1}. \tag{35}$$

The remaining in- and outputs of the interconnected model are

$$\begin{bmatrix} U_1 \\ U_2 \end{bmatrix} = \begin{bmatrix} U_1^k \\ U_2^{k+1} \end{bmatrix} \approx \begin{bmatrix} e_2(a_k) \\ -e_1(b_{k+1}) \end{bmatrix}, \ \begin{bmatrix} Y_1 \\ Y_2 \end{bmatrix} = \begin{bmatrix} Y_1^k \\ Y_2^{k+1} \end{bmatrix} \approx \begin{bmatrix} e_1(a_k) \\ e_2(b_{k+1}) \end{bmatrix}. \tag{36}$$

For a 2-segment discretization, two models of type (30), (31) are written one below each other, replacing conditions (35). Attaching another 1-segment model yields the 3-segment model, etc.

3.4 Collocated in-/outputs

The N-segment model on the spatial interval $[0, L]$ ($a_1 = 0$, $b_N = L$) with collocated in- and outputs

$$\begin{bmatrix} U_1 \\ U_2 \end{bmatrix} = \begin{bmatrix} U_1^1 \\ U_2^N \end{bmatrix} \approx \begin{bmatrix} e_2(0) \\ -e_1(L) \end{bmatrix}, \ \begin{bmatrix} Y_1 \\ Y_2 \end{bmatrix} = \begin{bmatrix} Y_1^1 \\ Y_2^N \end{bmatrix} \approx \begin{bmatrix} e_1(0) \\ e_2(L) \end{bmatrix}, \tag{37}$$

states and efforts $\boldsymbol{Z}, \boldsymbol{E} \in \mathbb{R}^{2N}$, is

$$\Sigma: \quad \begin{aligned} \dot{\boldsymbol{Z}} &= \boldsymbol{F}\boldsymbol{E} + \boldsymbol{G}\boldsymbol{U} \\ \boldsymbol{Y} &= \boldsymbol{G}^T\boldsymbol{E} + \boldsymbol{D}\boldsymbol{U}. \end{aligned} \tag{38}$$

The matrices $\boldsymbol{F} = \boldsymbol{F}^N$, $\boldsymbol{G} = \boldsymbol{G}^N$, $\boldsymbol{D} = \boldsymbol{D}^N$ are obtained from a recursive computation with $K = 2, \ldots, N$ [9]:

$$\boldsymbol{F}^K = \begin{bmatrix} \boldsymbol{F}^{K-1} & -\boldsymbol{g}_2^{K-1}(\boldsymbol{g}_1^1)^T \\ \boldsymbol{g}_1^1(\boldsymbol{g}_2^{K-1})^T & \boldsymbol{F}^1 \end{bmatrix}, \tag{39}$$

$$\boldsymbol{g}_1^K = \begin{bmatrix} \boldsymbol{g}_1^1 \\ -\boldsymbol{g}_1^{K-1} \end{bmatrix}, \quad \boldsymbol{g}_2^K = \begin{bmatrix} -\boldsymbol{g}_2^{K-1} \\ \boldsymbol{g}_2^1 \end{bmatrix}, \tag{40}$$

$$\boldsymbol{D}^K = -\boldsymbol{D}^{K-1} = \begin{bmatrix} 0 & -(-1)^K \\ (-1)^K & 0 \end{bmatrix}. \tag{41}$$

The matrices $\boldsymbol{F}$, $\boldsymbol{G}$, $\boldsymbol{D}$ define a Dirac structure (van der Schaft, 2000) between the flow variables $[\dot{\boldsymbol{Z}}^T \ \boldsymbol{Y}^T]^T$ and the efforts $[\boldsymbol{E}^T \ \boldsymbol{U}^T]^T$. This Dirac structure describes the power-conserving interconnection of the energy storing and dissipating elements in the discretized model. The employed discretization scheme approximates the total energy

$$H^N = \sum_{k=1}^{N} H_{a_k b_k} \approx H \tag{42}$$

and conserves the energy balance equation (9):

$$\dot{H}^N \leq Y_1 U_1 + Y_2 U_2 \approx e_1(0)e_2(0) - e_1(L)e_2(L). \tag{43}$$

The vector of efforts $\boldsymbol{E}$ is the gradient $\nabla_Z H^N(\boldsymbol{Z})$ of the approximate energy.

[9] The superscript K with the matrices $\boldsymbol{F}$, $\boldsymbol{g}_1$, $\boldsymbol{g}_2$ and $\boldsymbol{D}$ denotes the interconnection of K segments, whereas k with the in- and outputs refers to the k-th segment.

3.5 Non-collocated in-/outputs

The feedthrough in the model (38) allows to rewrite the equations in terms of the non-collocated pair of in- and outputs $\tilde{\boldsymbol{U}}$ and $\tilde{\boldsymbol{Y}}$ according to (12):

$$\tilde{\Sigma}: \quad \begin{aligned} \dot{\boldsymbol{Z}} &= \tilde{\boldsymbol{F}}\boldsymbol{E} + \tilde{\boldsymbol{G}}\tilde{\boldsymbol{U}} \\ \tilde{\boldsymbol{Y}} &= \tilde{\boldsymbol{H}}^T\boldsymbol{E} + \tilde{\boldsymbol{D}}\tilde{\boldsymbol{U}}, \end{aligned} \tag{44}$$

with

$$\begin{aligned} &\tilde{\boldsymbol{F}} = \boldsymbol{F} + (-1)^N \boldsymbol{g}_2 \boldsymbol{g}_1^T, \quad \tilde{\boldsymbol{G}} = \begin{bmatrix} \boldsymbol{g}_1 & -(-1)^N \boldsymbol{g}_2 \end{bmatrix}, \\ &\tilde{\boldsymbol{H}}^T = \begin{bmatrix} \boldsymbol{g}_2^T \\ (-1)^N \boldsymbol{g}_1^T \end{bmatrix}, \quad \tilde{\boldsymbol{D}} = \begin{bmatrix} (-1)^N & 0 \\ 0 & -(-1)^N \end{bmatrix}. \end{aligned} \tag{45}$$

3.6 Non-collocated in-/outputs, terminal resistance

A resistive relation (13) at $x = L$ can be written

$$U_2 = -\frac{Y_2}{R_L} = -\frac{\boldsymbol{g}_2^T\boldsymbol{E}}{R_L} - \frac{(-1)^N U_1}{R_L}. \tag{46}$$

Replacing this equation in the model of the N-segment discretized system (38) and taking the non-collocated output yields the SISO model

$$\bar{\Sigma}: \quad \begin{aligned} \dot{\boldsymbol{Z}} &= \bar{\boldsymbol{F}}\boldsymbol{E} + \bar{\boldsymbol{g}}U_1 \\ Y_2 &= \bar{\boldsymbol{h}}^T\boldsymbol{E} + \bar{d}U_1 \end{aligned} \tag{47}$$

with

$$\begin{aligned} &\bar{\boldsymbol{F}} = \boldsymbol{F} - \boldsymbol{g}_2\boldsymbol{g}_2^T/R_L, \quad &\bar{\boldsymbol{g}} = \boldsymbol{g}_1 - (-1)^N g_2/R_L, \\ &\bar{\boldsymbol{h}}^T = \boldsymbol{g}_2^T, &\bar{d} = (-1)^N. \end{aligned} \tag{48}$$

Remark 3. The case of collocated in- and outputs with terminal resistance is omitted. The stability of the inverse model, as discussed in the sequel, corresponds to the collocated MIMO case.

4. INVERSE MODELS

Due to the feedthrough term in the models Σ, $\tilde{\Sigma}$ and $\bar{\Sigma}$ it is straightforward to write down the corresponding inverse models (denoted with a prime).

4.1 Collocated in-/outputs

$$\Sigma': \quad \begin{aligned} \dot{\boldsymbol{Z}} &= \boldsymbol{F}'\boldsymbol{E} + \boldsymbol{G}'\boldsymbol{Y} \\ \boldsymbol{U} &= (\boldsymbol{G}')^T\boldsymbol{E} + \boldsymbol{D}'\boldsymbol{Y} \end{aligned} \tag{49}$$

with

$$\begin{aligned} &\boldsymbol{F}' = \boldsymbol{F} + \boldsymbol{G}\boldsymbol{D}\boldsymbol{G}^T, \\ &\boldsymbol{G}' = -\boldsymbol{G}\boldsymbol{D}, \qquad \boldsymbol{D}' = -\boldsymbol{D}. \end{aligned} \tag{50}$$

4.2 Non-collocated in-/outputs

$$\tilde{\Sigma}': \quad \begin{aligned} \dot{\boldsymbol{Z}} &= \tilde{\boldsymbol{F}}'\boldsymbol{E} + \tilde{\boldsymbol{G}}'\tilde{\boldsymbol{Y}} \\ \tilde{\boldsymbol{U}} &= (\tilde{\boldsymbol{H}}')^T\boldsymbol{E} + \tilde{\boldsymbol{D}}'\tilde{\boldsymbol{Y}} \end{aligned} \tag{51}$$

with

$$\begin{aligned} &\tilde{\boldsymbol{F}}' = \boldsymbol{F} - (-1)^N \boldsymbol{g}_1\boldsymbol{g}_2^T, \qquad \tilde{\boldsymbol{G}}' = \begin{bmatrix} (-1)^N \boldsymbol{g}_1 & \boldsymbol{g}_2 \end{bmatrix}, \\ &(\tilde{\boldsymbol{H}}')^T = \begin{bmatrix} -(-1)^N \boldsymbol{g}_2^T \\ \boldsymbol{g}_1^T \end{bmatrix}, \quad \tilde{\boldsymbol{D}}' = \tilde{\boldsymbol{D}}. \end{aligned} \tag{52}$$

4.3 Non-collocated in-/outputs, terminal resistance

$$\bar{\Sigma}' : \quad \begin{aligned} \dot{\boldsymbol{Z}} &= \bar{\boldsymbol{F}}'\boldsymbol{E} + \bar{\boldsymbol{g}}'Y_2 \\ U_1 &= (\bar{\boldsymbol{h}}')^T\boldsymbol{E} + \bar{d}'Y_2 \end{aligned} \tag{53}$$

with

$$\begin{aligned} \bar{\boldsymbol{F}}' &= \tilde{\boldsymbol{F}}', & \bar{\boldsymbol{g}}' &= (-1)^N\bar{\boldsymbol{g}}, \\ (\bar{\boldsymbol{h}}')^T &= -(-1)^N\bar{\boldsymbol{h}}^T & \bar{d}' &= \bar{d} = (-1)^N. \end{aligned} \tag{54}$$

5. FEEDFORWARD CONTROL

The following feedforward control problem is considered for the three different state representations:

Given a desired output trajectory $\boldsymbol{Y}_d(t)$ (or $\tilde{\boldsymbol{Y}}_d(t)$ or $Y_{2,d}(t)$), determine the corresponding input $\boldsymbol{U}_d(t)$ (or $\tilde{\boldsymbol{U}}_d(t)$ or $U_{1,d}(t)$) such that the output tracks the desired trajectory in the ideal, undisturbed case with appropriate initial conditions $\boldsymbol{Z}(0) = \boldsymbol{Z}_d(0)$.

The structure preserving discretization scheme as presented before leads to models with a feedthrough term such that the relative degree of the outputs $\boldsymbol{Y}(t)$ (or $\tilde{\boldsymbol{Y}}(t)$ or $Y_2(t)$) is zero. Impeding the (direct) application of the flatness-based approach, this structural property of the discretized models allows for a straightforward formulation of the inverse system, as seen above. The inverse system in the considered cases is exactly the zero dynamics (of full order $n = 2N$) of the original system, excited by the (desired) output. With the solution of the inverse dynamics, the state $\boldsymbol{Z}_d(t)$ along the desired output trajectory can be parameterized. Finally, the output equation can be solved for the desired input function $\boldsymbol{U}_d(t)$ (or $\tilde{\boldsymbol{U}}_d(t)$ or $U_{1,d}(t)$).

5.1 Collocated in-/outputs

In the case of collocated in- and outputs, due to skew-symmetry of $\boldsymbol{GDG}^T$, the original and the inverse system share the same dissipation matrix $\boldsymbol{R} = -\frac{1}{2}(\boldsymbol{F} + \boldsymbol{F}^T) = \boldsymbol{R}'$. The inverse model Σ' is nothing else than the discretized model of the pH system (4) with the alternative choice of in- and outputs (11). If $\boldsymbol{R}$ is positive definite (or $\boldsymbol{R}$ is positive semi-definite and the damping is pervasive), the control input can be determined for a desired output trajectory by stable numerical integration of Σ'.

5.2 Non-collocated in-/outputs

In the other cases of non-collocated in- and outputs the inverse system can be unstable (corresponding to non-minimum phase original dynamics), depending on the magnitude of dissipation. The problem at hand is then the stable inversion of a non-minimum phase system for which there exists a series of solution approaches. In Chen and Paden (1996) it is proposed to solve the corresponding "two point boundary value problem of the zero dynamics driven by the desired output" by finding trajectories which start on an unstable manifold and end on a stable manifold. A constructive procedure is presented in Devasia et al. (1996). In Graichen et al. (2005), it is described how to solve the boundary value problem using a numerical routine contained in Matlab.

Whether the inverse models $\tilde{\Sigma}'$ and $\bar{\Sigma}'$ are stable or not is determined by the dissipation matrix $\bar{\boldsymbol{R}}' = -\frac{1}{2}(\bar{\boldsymbol{F}}' + (\bar{\boldsymbol{F}}')^T) = \tilde{\boldsymbol{R}}'$ which has the following block matrix structure:

$$\bar{\boldsymbol{R}}' = \begin{bmatrix} \boldsymbol{A} & \boldsymbol{B} & -\boldsymbol{B} & \boldsymbol{B} & \dots \\ \boldsymbol{B} & \boldsymbol{A} & \boldsymbol{B} & -\boldsymbol{B} & \dots \\ -\boldsymbol{B} & \boldsymbol{B} & \boldsymbol{A} & \boldsymbol{B} & \\ \boldsymbol{B} & -\boldsymbol{B} & \boldsymbol{B} & \boldsymbol{A} & \\ \vdots & \vdots & & & \ddots \end{bmatrix}, \tag{55}$$

$$\boldsymbol{A} = \begin{bmatrix} R_1 & -2 \\ -2 & R_2 \end{bmatrix}, \quad \boldsymbol{B} = \begin{bmatrix} 0 & 2 \\ 2 & 0 \end{bmatrix}. \tag{56}$$

From the structure of $\boldsymbol{A}$ it is obvious that $R_1, R_2 > 0$, i. e. a fully damped system is indispensable for positive (semi-)definiteness of $\bar{\boldsymbol{R}}'$.

Lemma 1. The dissipation matrix $\bar{\boldsymbol{R}}'$ in Eq. (55) with $R_1, R_2 > 0$ is positive definite if and only if

$$R_1R_2 > (2N)^2 \tag{57}$$

with N the number of segments of the discretized model. □

Proof. $\bar{\boldsymbol{R}}'$ can be transformed into a block triangular matrix with a zero matrix $\boldsymbol{O}_{N\times N}$ in the lower left corner by pairwise permuting rows and columns, which preserves the definiteness property. The definiteness of the transformed matrix can be checked with the help of the Schur decomposition. Doing this subsequently for models with $K = 1, \dots, N$ segments, condition (57) follows. □

The lemma provides a condition for asymptotic stability of the inverse pH systems $\tilde{\Sigma}'$ and $\bar{\Sigma}'$. If the condition holds, a bounded control input corresponding to a desired (bounded) output trajectory can be determined by simple numerical integration.

Remark 4. Note that the bound for admissible dissipation increases with the number of segments N, while the values of R_i decrease when the segments become shorter. As a consequence, the condition can only be satisfied in heavily damped systems with a coarse spatial discretization.

Remark 5. The condition only depends on the matrices $\boldsymbol{F}$, $\boldsymbol{G}$ and $\boldsymbol{D}$ of the original model an not on the functional relations between efforts and states.

5.3 Main result

The observations on the structure of the discretized (inverse) port-Hamiltonian models with complete damping, i. e. $r_1, r_2 > 0$ ($R_1, R_2 > 0$, respectively) and the conclusions regarding the solution of the feedforward control problem can be summarized as follows:

Proposition 2. The feedforward control problem for the considered discretized distributed-parameter port-Hamiltonian transmision systems can be solved in the case of *collocated* in- and outputs by numerical integration of the *asymptotically stable* inverse (or dual) system Σ'.

In the case of *non-collocated* in- and outputs, the inverse system $\tilde{\Sigma}'$, (or $\bar{\Sigma}'$ if there is a terminal resistance) is asymptotically stable if and only if condition (57) holds. Only in this case a simple numerical integration of the inverse dynamics yields a bounded input trajectory for a given bounded desired output. □

6. CONCLUSIONS AND FUTURE WORK

The feedforward control problem for finite-dimensional port-Hamiltonian approximations of nonlinear hyperbolic systems of two conservation laws ("transmission systems") has been discussed. The models which are obtained from a structure preserving spatial discretization possess a feedthrough term which allows to express the inverse system in a straightforward way. While the inverse model with collocated in- and outputs is stable, and hence, a feedforward controller easy to determine by numerical integration, this property is in general lost in the non-collocated case. A condition for admissible damping in this case has been derived, which is violated for sensible physical systems. Then, to solve the feedforward control problem, methods for the stable inversion of non-minimum phase systems have to be employed.

The approach which is sketched in this paper exploits the structure of the discretized models with a particular choice of shape functions. Ongoing work is on adopting the procedure in Devasia et al. (1996) for the stable inversion of the discussed models in the non-minimum phase case.

Different shape functions lead to models of different structure, e. g. with full relative degree, for which the flatness-based approach is more suitable. The main difficulty then is the symbolic expression of the differential parameterizations of states and inputs for fully damped, nonlinear systems. Also other numerical methods, e. g. based on the method of characteristics, will be taken into account for comparison with the proposed scheme.

Future work is planned on exploiting the modular, port-Hamiltonian structure of the discretized models in order to find efficient numerical methods to solve the feedforward control problem. Further issues are the application to flexible mechanical structures and to nonlinear transmission networks.

ACKNOWLEDGEMENTS

The author thanks Jacquelien Scherpen and Arjan van der Schaft for the fruitful discussions during his stay in Groningen, as well as the reviewers for the helpful comments.

REFERENCES

Chen, D. and Paden, B. (1996). Stable inversion of nonlinear non-minimum phase systems. *Int. J. Control*, 64, 81–97.

Devasia, S., Chen, D., and Paden, B. (1996). Nonlinear inversion-based output tracking. *IEEE Trans. Automat. Control*, 41(7), 930–942.

Farle, O., Klis, D., Jochum, M., Floch, O., and Dyczij-Edlinger, R. (2013). A port-Hamiltonian finite-element formulation for the Maxwell equations. In *Proc. Int. Conf. Electromagnetics in Advanced Applications (ICEAA)*, 324–327.

Fliess, M., Martin, P., Petit, N., and Rouchon, P. (1999). Active signal restoration for the telegraph equation. In *Proc. 38th IEEE Conf. on Decision and Control (CDC)*, volume 2, 1107–1111.

Golo, G., Talasila, V., van Der Schaft, A., and Maschke, B. (2004). Hamiltonian discretization of boundary control systems. *Automatica*, 40(5), 757–771.

Graichen, K., Hagenmeyer, V., and Zeitz, M. (2005). A new approach to inversion-based feedforward control design for nonlinear systems. *Automatica*, 41, 2033–2041.

Hamroun, B., Lefèvre, L., and Mendes, E. (2006). Port-based modelling for open channel irrigation systems. In *Proc. Int. Conf. Water Resources, Hydraulics & Hydrology, Portoroz, Slovenia*, 41–46.

Knüppel, T., Woittennek, F., and Rudolph, J. (2010). Flatness-based trajectory planning for the shallow water equations. In *Proc. 49th IEEE Conf. on Decision and Control (CDC)*, 2960–2965.

Macchelli, A. and Melchiorri, C. (2005). Control by interconnection of mixed Port Hamiltonian systems. *IEEE Trans. Automat. Contr.*, 50(11), 1839–1844.

Moulla, R., Lefèvre, L., and Maschke, B. (2012). Pseudo-spectral methods for the spatial symplectic reduction of open systems of conservation laws. *Journal of Computational Physics*, 231(4), 1272–1292.

Pasumarthy, R. and van der Schaft, A. (2006). A finite dimensional approximation of the shallow water equations: The port-Hamiltonian approach. In *Proc. 45th IEEE Conf. Decision and Control (CDC)*, 3984–3989.

Schmuck, C., Woittennek, F., Gensior, A., and Rudolph, J. (2014). Feed-forward control of an HVDC power transmission network. *IEEE Trans. Contr. Syst. Tech.*, 22(2), 597–606.

Schöberl, M. and Siuka, A. (2013). On Casimir functionals for infinite-dimensional Port-Hamiltonian control systems. *IEEE Trans. Automat. Contr.*, 58(7), 1823–1828.

van der Schaft, A.J. (2000). *L2-Gain and Passivity Techniques in Nonlinear Control*. Springer-Verlag, London.

van der Schaft, A.J. (2006). Port-Hamiltonian systems: an introductory survey. In *Proc. Int. Congress of Mathematicians, Madrid*, 1339–1365.

van der Schaft, A.J. and Maschke, B.M. (2002). Hamiltonian formulation of distributed-parameter systems with boundary energy flow. *J. Geometry and Physics*, 42(1), 166–194.